Corrole basicity in the excited states: Insights on structure-property relationships

Kruk, Mikalai M.; Klenitsky, Dmitry, V; Gladkov, Lev L. & MAES, Wouter (2020)
Corrole basicity in the excited states: Insights on structure-property relationships. In:
JOURNAL OF PORPHYRINS AND PHTHALOCYANINES, 24 (5-7) , p. 765 -774.

DOI: 10.1142/S1088424619501797
Handle: http://hdl.handle.net/1942/31795

Corrole basicity in the excited states: insights on structure-property relationships@

Mikalai M. Kruk*[a], Dmitry V. Klenitsky[a], Lev L. Gladkov[b], Wouter Maes*[c]

[a] *Belarusian State Technological University, Sverdlov Str., 13a, 220006, Minsk, Belarus*

[b] *Belarusian State Academy of Communications, F. Skorina Str., 8/2, 220114, Minsk, Belarus*

[c] *Institute for Materials Research (IMO-IMOMEC), Hasselt University, Agoralaan 1, B-3590, Diepenbeek, Belgium*

Received date (to be automatically inserted after your manuscript is submitted)
Accepted date (to be automatically inserted after your manuscript is accepted)

ABSTRACT: Steady-state fluorescence measurements and quantum-chemical DFT geometry optimizations are applied to extend the structure-property relationships between the free base corrole macrocycle conformation and its basicity to the lowest excited S_1 and T_1 states. Direct basicity estimation in the lowest excited S_1 state is demonstrated by means of fluorescence quantum yield measurements. The long wavelength T1 tautomer is found to retain its basicity in the S_1 state, whereas the short wavelength T2 tautomer shows a noticeable decrease in basicity in the S_1 state, which is related to the in-plane tilting of the pyrrole ring to be protonated. The conformational changes upon going from the ground to the lowest excited T_1 state and the influence of the *meso*-aryl substitution pattern on the overall degree of distortions and tilting of the pyrrole ring to be protonated are also discussed from the point of view of macrocycle basicity.

KEYWORDS: free base corroles, NH tautomers, basicity, excited states, fluorescence, macrocycle distortions, pyrrole tilting

*Correspondence to:
Prof. Wouter Maes, Institute for Materials Research (IMO-IMOMEC), Hasselt University, Agoralaan 1, B-3590, Diepenbeek, Belgium, Fax: (+32) 11 268299; Tel: (+32) 11 268312; E-mail: wouter.maes@uhasselt.be
Prof. Mikalai M. Kruk, Belarusian State Technological University, Physics Department, Sverdlov Str., 13a, 220006, Minsk, Belarus, Fax: (+375) 17 3276217; Tel: (+375) 17 3994960; E-mail: krukmikalai@yahoo.com, m.kruk@belstu.by

@ This paper is dedicated to Professor Roberto Paolesse in connection with his 60th anniversary.

INTRODUCTION

Tetrapyrrolic macrocycles are known to display both basic and acidic properties, which results in proton(s) binding or dissociation under appropriate conditions. Macrocycle basicity has been studied repeatedly for a large number of porphyrin derivatives differing in their peripheral substitution pattern, with the main attention being devoted to the structural features of doubly protonated species [1-10 and refs. therein]. The pronounced nonplanar macrocycle distortions observed for doubly protonated porphyrins render these compounds useful model systems for studies on the relationship between the type and degree of macrocycle distortions and different physico-chemical porphyrinoid properties. The nonplanar distortion of the porphyrin macrocycle was found to increase both the basicity of the pyrrolenine nitrogen atoms and the acidity of the pyrrole NH protons quite dramatically [5]. These features can be explained by tilting of the pyrrole and pyrrolenine rings out of the macrocycle plane, leading to the exposure of the pyrrolenine nitrogen lone pair and pyrrole NH groups to the bulk solvent, thus facilitating intermolecular interactions.

<Figure 1 here>

In corroles, one pair of adjacent pyrrolic rings is bound directly through a C_a-C_a bond due to the lack of one C_m atom, thus forming a contracted macrocycle (see Figure 1). The aromatic stabilization in such a contracted macrocycle is achieved by the increase in the number of pyrrole rings at the expense of pyrrolenines, thus keeping the number of π-electrons the same as in porphyrins. As a result, the corrole macrocycle consists of three pyrrole and one pyrrolenine ring rather than two pyrrole and two pyrrolenine rings in free base (i.e. non-metalated) porphyrins. The decrease in the macrocycle core size and the increase in the number of pyrrole NH protons are considered to be the two main reasons which ultimately lead to the nonplanar macrocycle conformation in free base corroles. The corrole macrocycle has pronounced out of plane distortions, even when the sterical strains imposed by the peripheral substitution are absent [11,12]. The asymmetry of the corrole macrocycle results in different tilting angles of individual pyrrole/pyrrolenine rings relative to the mean macrocycle plane [12], and this feature was proposed to account for the different basicity of individual pyrrolenine rings. This has been demonstrated explicitly through spectrophotometric titration experiments [13], wherein the protonated corrole species was found to form via two parallel ways with different rates. Due to efficient ground state NH tautomerization, the ring to be protonated is different for the two corrole NH tautomers (Figure 1), i.e. the long wavelength and short wavelength T1 and T2 tautomers with proton-free rings D and C, respectively [13,14]. Based on the calculated tilting angles, the higher basicity was assigned to the T1 tautomer because of the larger tilt angle of ring D, while the lower basicity was assigned to the T2 tautomer due to the lower tilt angle of ring C [13]. These findings have been supported afterwards by DFT geometry optimizations and *ab initio* molecular dynamic simulations, which demonstrated that the nitrogen atom of the pyrrole ring to be protonated is not only tilted stronger, but it is also substantially more accessible for protons in case of the T1 tautomer as compared to the T2 tautomer [14]. Distribution of the electrostatic potential over the corrole macrocycle was shown to facilitate proton binding by the T1 tautomer as well, but the structural factors play the major role [14].

The pK_a value for pyrrolenine nitrogen protonation can vary noticeably in case of peripheral substitution with electron-donating or electron-withdrawing groups at the C_m or C_b carbon atoms of the corrole macrocycle [15-19]. Gross et al. suggested that formation of the monoprotonated corrole species (H_3Cor □ H_4Cor^+) can be related to the second protonation step in porphyrins, i.e. H_3P^+ □ H_4P^{2+}, due to the similar structural features of free base corroles and monoprotonated porphyrins [15]. It was proposed that for both macrocycles the major steric penalty is paid upon adding the first proton. The formal charge of the molecules is not so much of importance, but the number of NH protons in the macrocycle core is. However, recent quantum-mechanical and *ab initio* molecular dynamic simulation studies demonstrated that the rate of the second protonation step in porphyrins depends strongly on the interplay between the

nonplanar macrocycle distortions and the electrostatic potential of the binding site [20]. Meanwhile, the hypothesis of Gross et al. enables to explain qualitatively the huge increase in acidity of free base corroles as compared to porphyrins with the same peripheral substitution pattern (both *meso*- and pyrrole-substituted), whereas their basicity constants are very close to each other.

A characteristic feature of nonplanar tetrapyrrolic compounds is the large Stokes shift of the fluorescence signal, which is due to conformational rearrangements in the excited singlet S_1 state [21,22]. The mean value of the macrocycle atom displacement Δ23 (*vide infra*) for the ground state of free base corroles varies from 0.15 Å in the pristine unsubstituted corrole up to 0.503 Å in undecasubstituted 2,3,7,8,12,12,17,18-octabromo-5,10,15-tris(pentafluorophenyl)corrole [23,24]. Thus, for free base 5,10,15-triarylcorroles, whose Δ23 values range from 0.20 to 0.25 Å, substantial conformational flexibility may be suggested. Upon photoexcitation, redistribution of the electronic density takes place and one can expect changes in the molecular conformation, which would lead to the alteration of the basicity of the pyrrolic NH protons. Recently, it was demonstrated that the Δ23 value, which is characteristic for the molecular conformation as a whole, does not always run in parallel with the local conformational changes of the macrocycle [25], which, as has been indicated above, plays a crucial role in the macrocycle basicity. It was pointed out by Kadish et al. that the basicity of triaryl-substituted corroles with a varying degree of sterical hindrance induced by the aryl substituents is different [16-19]. *Meso*-aryl-substituted corroles have a distinctly different basicity than C_b-alkyl-substituted corroles [26,27]. These results seem to point to an important role for *meso*-aryl substitution in the stabilization of the corrole macrocycle conformation.

In this paper we report on our studies on structure-property relationships to understand the basicity of free base corroles in their lowest excited S_1 and T_1 states. Steady-state fluorescence measurements and quantum-chemical (DFT) geometry optimization have been carried out for the ground and exited states of 10-(4,6-dichloropyrimidinyl)-5,15-dimesitylcorrole (hereafter referred as the H_3AB_2 corrole), for which extensive data on the ground state acid-base equilibria have been gathered earlier [13]. We present experimental data on the basicity of the lowest excited S_1 state and discuss the molecular conformational changes upon photoexcitation. Then, the analysis of the molecular conformation of the H_3AB_2 corrole in the lowest triplet T_1 state is presented and its basicity is compared to both ground S_0 and lowest excited S_1 states. Finally, we discuss the influence of the *meso*-aryl substituents on the ground and excited state basicity of free base corroles by comparison of their molecular conformations.

EXPERIMENTAL

Synthesis of the 10-(4,6-dichloropyrimidin-5-yl)-5,15-dimesitylcorrole (H_3AB_2) was carried out in accordance with a previously published synthetic procedure [28,29]. Ground state absorption and steady state fluorescence spectra were measured with a spectrofluorometer SM 2203 (JSC “Solar”, Belarus) equipped with a temperature-controlled cell holder at 298 K. The sample emission was measured at a right angle to the excitation light. The concentrations of the corrole solutions in ethanol did not exceed $1.0 \cdot 10^{-5}$ M and were measured spectrophotometrically by means of known extinction coefficients at 298 K: λ_{max}/nm (log ε/$M^{-1}cm^{-1}$) 410 (5.02), 427 (4.92), 570 (4.30), 599 (4.05) and 635 (3.28) for the free base H_3AB_2 corrole, and 421 (5.07), 533 (3.77), 597 (3.87) and 644 (4.56) for the protonated $H_4AB_2^+$ corrole [13]. The samples were handled in standard spectroscopic rectangular quartz 1×1 cm cells with a tight stopper. Fluorescence quantum yield (Φ_{fl}) values were determined with the standard sample method, using free base 5,10,15,20-tetraphenylporphyrin (Φ^0_{fl} = 0.09 [30]) as a standard.

The solvent used was purified with a standard procedure [31]. The choice for ethanol as the solvent for the titration was based on the fact that it is inert toward tetrapyrrolic macrocycles and exhibits the properties of a weak acid and a weak base simultaneously. A solution of sulfuric acid in ethanol was used as the titrant. The titrant concentration was chosen as such that the total volume changes of the solution by the end of the titration procedure did not exceed 5%. The measured spectra were corrected for the dilution of the solution. The ethanol-sulfuric acid system was studied previously in the range of acid concentrations from 0.01 to 11.22 M, and the dependence of the acidity function H_0 (Hammett constant), which characterizes the proton donating power of the medium, on the sulfuric acid concentration was evaluated [13].

The 7C plane [32,33], given by the least-square distances to carbon atoms C_1, C_4, C_5, C_6, C_9, C_{16} and C_{19}, was used as the mean macrocycle plane. The overall degree of macrocycle distortions was taken as the Δ23 value:

$$\Delta 23 = \sqrt{\frac{1}{23}\sum_{i=1}^{23}\Delta z_i^2}\ ,$$

where Δz_i is the deviation for the *i*-th atom of the macrocycle from the mean plane.

Molecular geometry optimizations of the ground singlet S_0 and lowest excited triplet T_1 states of the two corrole NH tautomers of the studied free base corroles and the normal modes were carried out using density functional theory (DFT) with the PBE exchange-correlation functional and the three-exponent basis set 3z using the algorithm implemented in the quantum chemical program Priroda [34,35]. At first, the molecular geometries were optimized. Then, normal modes were calculated for the optimized molecular geometries and the absence of imaginary values for the mode frequencies served as a criterion for the stationary point.

RESULTS AND DISCUSSION

Fluorescence titration of 10-(4,6-dichloropyrimidin-5-yl)-5,15-dimesitylcorrole (H_3AB_2)

The fluorescence spectra for a corrole solution of H_3AB_2 measured over the course of the titration experiment are shown in Figure 2a. One can see that an increase in sulfuric acid concentration in the sample solution leads to a decrease in the intensity of the bands with maxima at 606 and 644.5 nm, which belong to fluorescence originating from the T2 and T1 tautomer of the free base H_3AB_2 corrole, respectively. Simultaneously, a new broad fluorescence band with a maximum at 675 nm appears in the spectrum due to the formation of the monoprotonated $H_4AB_2^+$ corrole. The observed broadening of the fluorescence spectrum is in line with earlier observations for mono- and doubly protonated porphyrins [6], and should be related to both the degree of nonplanar macrocycle distortions and the increase of the conformational degree of freedom, the latter promoting out-of-plane vibrational modes [36]. The Stokes shift for $H_4AB_2^+$, calculated as the difference in the energy of the 0-0 band maxima in the absorption and fluorescence spectra, is 713 cm^{-1}. Such a value is indicative for substantial conformational rearrangements in the excited S_1 state of the monoprotonated species as compared to those expected for the T1 and T2 free base corrole tautomers, for which the Stokes shifts are 233 and 192 cm^{-1}, respectively.

<Fig. 2 here>

According to the model of parallel protonation of tautomer T1 and T2, whose protonation constant ratio is χ [13], one can write that:

$$\frac{T1}{T1_0} = \left(\frac{T2}{T2_0}\right)^{\chi} \text{ and } \frac{T2}{T2_0} = \left(\frac{T1}{T1_0}\right)^{1/\chi}, \qquad (1.1–1.2)$$

where the fractions $\frac{T1}{T1_0}$ and $\frac{T2}{T2_0}$ represent the residual ratios of tautomer concentrations at each protonation step to their initial concentrations. This means that the proportion of the concentrations of the T1 and T2 tautomers in the lowest singlet excited S_1 state will vary during the protonation procedure. Indeed, the plot of the peak fluorescence intensity at 644.5 nm as a function of the peak fluorescence intensity at 606 nm has a slightly concave shape (Figure 2b). This observation is in line with our previous finding derived from the ground state absorption titration data that the protonation of the T1 tautomer occurs faster than for the T2 tautomer [13].

A fluorescence quantum yield of 0.076 was determined for the free base H_3AB_2 corrole solution in ethanol at 298 K. This figure is an average value over the two corrole NH tautomers as their individual fluorescence quantum yield values differ [37]. $\Phi_{fl} = 0.045 \pm 0.01$ has been measured for the T1 tautomer and this value was shown to be independent of temperature [37], whereas that of the T2 tautomer revealed a strong temperature dependence due to efficient NH tautomerization in the lowest excited singlet S_1 state [37,38]. Using a mathematical model describing the excitation energy deactivation of the lowest excited state of the T2 tautomer, temperature dependence of the fluorescence quantum yield has been noticed, giving rise to a Φ_{fl} value of 0.095 ± 0.01 at 298 K [38]. Taking into account the equal probability of S_1 state population upon excitation into the isosbestic point, the Φ_{fl} value for the T1 tautomer was calculated to be 0.056 ± 0.01, which agrees rather well with the above mentioned experimental value. Formation of the monoprotonated $H_4AB_2^+$ corrole results in an increase of the fluorescence intensity. The fluorescence quantum yield of the monoprotonated $H_4AB_2^+$ species in ethanol reveals an almost two-fold increase, up to 0.126. The fluorescence quantum yield shows two distinct steps when plotted as a function of the sulfuric acid concentration added to the solution (Figure 3). The sharp increase in fluorescence quantum yield at the start of the titration (up to a sulfuric acid concentration of $\sim 1.0 \cdot 10^{-4}$ M) should mainly be related to the formation of the $H_4AB_2^+$ corrole by protonation of the T1 tautomer, whereas the gently sloping second step accounts for the slower protonation of the T2 tautomer. One needs to keep in mind that both tautomers coexist during the whole titration procedure, but a higher proportion of the T1 tautomer is consumed at the start of the protonation process, whereas at the terminal states a higher proportion of the T2 tautomer is protonated.

<Fig.3 here>

Basicity of the NH tautomers in the lowest excited singlet S_1 state and structural prerequisites for basicity changes

The fluorescence intensity as measured in the titration experiments is proportional to the fluorescence intensity of the initial species, i.e. the two NH tautomers of the free base H_3AB_2 corrole and the monoprotonated $H_4AB_2^+$ corrole. Each of these species has its own fluorescence quantum yield. The measured fluorescence quantum yield is hence proportional to the sum of those contributions, i.e. $\Phi_{fl} \sim \Phi_{fl}(T1)[H_3AB_2(T1)] + \Phi_{fl}(T2)[H_3AB_2(T2)] + \Phi_{fl}(P)[H_4AB_2^+]$. Taking into account that the averaged fluorescence quantum yield values fall within a 10% range of fractional error when the NH tautomer ratio varies from 3/7 to 7/3 (this range is higher than the ratio expected at the last stages of the titration experiments [13]), the above trinomial can be reduced to a two term function: $\Phi_{fl}(FB)[H_3AB_2(T1+T2)] + \Phi_{fl}(P)[H_4AB_2^+]$. When the total concentration of emissive species equals the sum $[H_3AB_2(T1+T2)] + [H_4AB_2^+]$, the fluorescence quantum yield is in direct proportion to the concentration of the monoprotonated species (Figure 3, inset). The experimental fluorescence quantum yield dependence on acid concentration can easily be transformed into a dependence of the relative concentration of the monoprotonated corrole $[H_4AB_2^+]/[H_4AB_2^+]_{max}$ in the lowest excited singlet S_1 state on acid concentration (Figure 4, black triangles). The relative concentration of the monoprotonated corrole in the ground singlet S_0 state is directly derived from the spectra measured upon spectrophotometric titration as

the ratio of the absorbance at the maximum of the 0-0 band during the titration to the absorbance after complete conversion of the free base molecules to the monoprotonated species (Figure 4, white triangles).

<Fig. 4 here>

Comparison of the two superimposed plots shown in Figure 4 allows to make unambiguous conclusions about the basicity in the lowest singlet S_1 state as compared to that in the ground S_0 state. One can see that the data points for the faster stage of the protonation, corresponding to the equilibrium H_3AB_2(T1) $\rightleftharpoons$ $H_4AB_2^+$, overlap. This indicates that the corresponding basicity value of the T1 tautomer remains unchanged upon photoexcitation to the lowest singlet S_1 state. The amounts of the protonated molecules at higher acid concentrations do reveal a difference between the ground singlet S_0 and excited singlet S_1 states. Formation of the $H_4AB_2^+$ corrole species occurs faster in the ground state. This means that the equilibrium H_3AB_2(T2) $\rightleftharpoons$ $H_4AB_2^+$ shifts in the direction of the free base H_3AB_2 corroles in the lowest singlet S_1 state, i.e. the ground S_0 state of the T2 tautomer has a higher basicity as compared to its lowest excited singlet S_0 state.

The different basicity of the two corrole NH tautomers can be explained by referring to the critical contribution of the molecular geometry [13,14]. In a planar macrocycle the nitrogen lone pair of the pyrrole ring to be protonated is barely accessible for intermolecular interactions due to shielding by the macrocycle core. When this ring undergoes out-of-plane tilting, the pyrrole nitrogen atom becomes accessible for any kind of intermolecular interactions in the solvent. Such a 'deshielding' was proposed to be the reason for the enhanced basicity of highly distorted nonplanar porphyrins [5] and free base corroles, whose macrocycle is intrinsically nonplanar. The two corrole NH tautomers have a distinctly different tilting of the pyrrole ring relative to the mean macrocycle plane [32,33]. Based on the DFT optimized molecular geometry [32], the tilting angle of pyrrole D in the T1 tautomer was calculated to be 6.7º, whereas the tilting angle for pyrrole C in the T2 tautomer was 3.9º [33]. Such a difference is supposed to account for the different basicity of the two NH tautomers in the electronic singlet S_0 ground state. This structure-property relationship we now apply to rationalize the macrocycle basicity in the lowest excited singlet S_1 state (Figure 4). In this framework, the same value for the basicity of the T1 tautomer in the ground and lowest excited singlet states is indicative for the negligible changes in macrocycle conformation, at least in the macroring quadrant containing pyrrole ring D. The absence of large conformational changes in the excited singlet S_1 state for both corrole NH tautomers is supported by the moderate value of the Stokes shift (see above). The T2 tautomer reveals a decrease in basicity in the excited singlet S_1 state as compared to the ground state, which is expected due to the smaller tilting angle of pyrrole ring C.

Molecular conformations of the corrole NH tatomers in the lowest triplet T_1 state and implications for basicity

Considering the prospects of photochemical applications of metal free corrole macrocycles, where intermolecular interactions occur in the electronic excited states, the properties of those molecules in the long living triplet state play a key role. The catalytic activity of free base tetrapyrrolic macrocycles revealed recently [39,40] may be substantially altered in the excited state, since this activity was postulated to relate to the degree of nonplanar macrocycle distortions which enable the core NH protons and the nitrogen lone pairs to be exposed out of the macrocycle plane, thus facilitating intermolecular contacts. Thus, inactive compounds in the ground state can become active when the excited states are populated and *vice versa*. The concentration of molecules in the lowest excited triplet T_1 state can be measured either with the transient triplet-triplet absorption or the phosphorescence technique. Being an excellent tool for the studies of the dynamics of excitation energy relaxation, the triplet-triplet absorption (T-T absorption) method is not the best choice for the exact evaluation of the concentrations of excited species. The T-T absorption spectra of tetrapyrrolic compounds are not characteristic, so the possibility to discriminate between the different absorbing species

is limited. The necessity to know the exact extinction coefficients of the T-T absorption bands adds a lot to these limitations. On the other hand, the phosphorescence of free base corroles is weak – to date the reported quantum yields do not exceed $1.7 \cdot 10^{-3}$ – and is observed at temperatures of 77 K and lower [41]. In addition, it was reported that due to suppression of the NH tautomerization rate at low temperature, a single rather than both tautomers populate the triplet state [41]. Thus, spectroscopic techniques at room temperature are not appropriate for acid-base equlibria measurements in the excited triplet T_1 state. One needs to search for a back-of-an-envelope method to estimate the basicity in the excited triplet T_1 state. Projection of the established structure-property relationships on the triplet states seems to be a reasonable way.

Our recent preliminary communication on the molecular conformation of free base corroles in the lowest triplet T_1 state unambiguously demonstrates an increase in the degree of out-of-plane macrocycle distortions upon photoexcitation [42]. Compared to the electronic singlet S_0 ground state, where both NH tautomers revealed the same Δ23 value (0.198 and 0.200 Å), both the type and the degree of distortions differ between the two corrole NH tautomers in the triplet T_1 state (Figure 5 and Table 1). The T1 tautomer has *wave* type distortions amounting to a Δ23 value of 0.330 Å, while the T2 tautomer has boundary (somewhat mixed *saddle-wave*) type distortions with a Δ23 value of 0.246 Å.

<Fig. 5 here>

<Table 1 here>

What happens if we apply the relationship between the tilt angle of the pyrrole ring to be protonated and the basicity of the macrocycle to the lowest triplet T_1 state? The pyrrole C tilting angle of 4º in the T2 tautomer remains practically the same as it was in the electronic ground state. Its neighboring ring D lies almost in the mean macrocycle plane, thus adding to the shielding of pyrrole C from the bulk solvent. These two structural factors decrease the basicity. On the contrary, the tilt of pyrroles A and B increases, rendering ring C more accessible. Taking into account the moderate increase in the overall degree of nonplanar distortions based on the Δ23 values (Table 1), one can expect a very small increase in basicity, if any. As for the T1 tautomer, the overall increase in the degree of nonplanar distortions (the Δ23 value rises to 0.330 Å) seems to overcome the slight decrease in the pyrrole ring D tilting down to 4.5 Å. As a result, one can expect a small increase in the basicity due to deshielding of the protonation site in such a distorted macrocycle.

Influence of the substitution pattern on the macrocycle conformation and basicity

Meso-substituted and β-alkylated free base corroles differ quite strongly in their acidity and basicity [26]. This feature parallels with that observed for porphyrins with the same peripheral substitution architecture. The sterically hindering mesityl and 4,6-dichloropyrimidinyl groups of H_3AB_2 promote nonplanar macrocycle distortions. The calculated Δ23 values for the ground S_0 state of the unsubstituted corrole macrocycle decrease as compared to those of the triaryl-substituted molecules, amounting to 0.163 and 0.152 Å for the T1 and T2 tautomers, respectively (Figure 6 and Table 1). Thus, the overall accessibility of both the NH protons and the nitrogen lone pairs of the pyrrole/pyrrolenine rings decreases as compared to that of the *meso*-aryl-substituted derivatives. All tilt angles (see Table 1) decrease as compared to the values found for the tri-aryl-substituted H_3AB_2 corrole. One can conclude that *meso*-free corrole derivatives possess a decreased basicity.

<Fig. 6 here>

The degree of nonplanar macrocycle distortions increases upon population of the excited triplet T_1 state and the Δ23 values amount to 0.209 and 0.204 Å for the T1 and T2 tautomer, respectively. These figures are about the same for the two NH tautomers and close to the values reported for the ground S_0 state of the *meso*-aryl substituted corrole. The type

of nonplanar macrocycle distortions differs for the two NH tautomers. For the T1 tautomer, a *wave*-type distortion is observed, whereas the clear alternative up and down tilting of the pyrrole rings in the T2 tautomer indicates the formation of a *saddl*e-type distorted macrocycle. The *meso*-aryl-substitution pattern promotes the nonplanar macrocycle distortions in both the ground S_0 and lowest excited T_1 triplet states and tends to switch the type of distortions in the triplet state, since for the tri-aryl-substituted H_3AB_2 corrole a mixed *saddle-wave* distortion type was found (see above). At the same time one can see that the T1 tautomer in the triplet T_1 state deviates more strongly from planarity than the T2 tautomer, giving rise to differences in the acid-base properties of the studied *meso*-aryl-substituted compound. Therefore, the unsubstituted macrocycle (the conclusion is likely to be valid for β-alkylated derivatives as well) has an equal accessibility of the macrocycle core (the Δ23 values are almost the same) and any difference in basicity could be due to a difference in the tilting angles of the pyrrole rings to be protonated. The tilting of ring D in the T1 tautomer is three times smaller as compared to that in the electronic ground state (1.9º versus 5.9º). Therefore, *meso*-free corroles in the lowest triplet T_1 state should definitely be less basic as compared to the ground state.

The T2 tautomer should be substantially less basic than the T1 tautomer, as evident from the in-plane tilting of the pyrrole ring to be protonated and the adjacent pyrrole rings (Table 1). As a result, the accessibility for the molecules from the bulk solvent decreases and such a relationship holds in both the ground singlet S_0 and lowest excited triplet T_1 state. Comparing the molecular geometries of *meso*-aryl-substituted and unsubstituted corroles, one can suggest an intrinsically lower basicity of the T2 tautomer as compared to the T1 tautomer.

CONCLUSIONS

The basicity in the lowest excited S_1 state of 10-(4,6-dichloropyrimidinyl)-5,15-dimesitylcorrole has been evaluated by steady-state fluorescence spectroscopy. It was found that the basicity of the T1 tautomer remains essentially the same as it was in the ground S_0 state, while the basicity of the T2 tautomer noticeably decreases. Based on the structure-property relationships between the tilting angle of the pyrrole ring undergoing protonation and its basicity, in-plane movement of the unprotonated pyrrole ring in the excited S_1 state is expected. The macrocycle conformation in the lowest excited T_1 state reveals two opposite trends: the pyrrole rings to be protonated adopt a more in-plane conformation, whereas the total out of plane macrocycle distortion increases. Thus, the basicity in the lowest excited T_1 state reflects the competition between these trends. *Meso*-aryl substitution leads to an increase in both the overall degree of nonplanar macrocycle distortion in the ground S_0 and lowest excited T_1 states and the out of plane tilting of the pyrrole ring to be protonated, thus providing conditions for an increase in the basicity of the macrocycle. Further studies aiming to quantify the discussed structure-property relationships are in progress.

Acknowledgements

Prof. W. Maes acknowledges the Research Foundation – Flanders (FWO) and Hasselt University for financial support. Prof. M. Kruk, Prof. L. Gladkov and Ass. Prof. D. Klenitsky acknowledge the State Program of Scientific Researches of the Republic of Belarus “Photonics, opto- and microelectronics”, grant no.1.3.01, for financial support.

REFERENCES

1. Stone A, Fleischner EB. *J. Am. Chem. Soc.* 1968; **90**: 2735 – 2748.
2. Ogoshi H, Watanabe E, Youshida Z. *Tetrahedron* 1973; **29**: 3241 – 3245.
3. Senge O, Forsyth T, Nguyen LT, Smith KM. *Angew. Chem. Int. Ed. Engl*. 1994; **33**: 2485 – 2487.
4. Senge MO, Kalish WW. *Z. Naturforsch. B* 1999; **54**: 943 – 959.

5. Takeda J, Sano M. *Chem. Lett*. 1995; **11**: 971 – 972.
6. Knyukshto VN, Solovyov KN, Egorova GD. *Biospectrosc*. 1998; **4**: 121 – 133.
7. Rosa A, Ricciardi G, Baerends EJ, Romeo A, Scolaro LM. *J. Phys. Chem. A*. 2003; **107**: 11468 – 11482.
8. Rosa A, Ricciardi G, Baerends EJ. *J. Phys. Chem. A* 2006; **110**: 5180 – 5190.
9. Cheng B, Munro OQ, Marques HM, Scheidt WR. *J. Am. Chem. Soc*. 1997; **119**: 10732 – 10742.
10. Kruk MM, Starukhin AS, Maes W. *Macroheterocycles* 2011; **4**: 69 – 79.
11. Harrison HR, Hodder OJR, Hodgkin DC. *J. Chem. Soc. (B)* 1971; 640 – 645.
12. Kruk MM, Klenitky DV, Maes W. *Macroheterocycles* 2019; **12**: 58 – 67.
13. Ivanova YuB, Savva VA, Mamardashvili NZh, Starukhin AS, Ngo TH, Dehaen W, Maes W, Kruk MM. *J. Phys. Chem. A*. 2012; **116**: 10683 – 10694.
14. Beenken W, Maes W, Kruk M, Martinez T. Presselt M. *J. Phys. Chem. A*. 2015; **119**: 6785 – 6883.
15. Mahammed A, Weaver JJ, Gray HB, Abdelas M, Gross Z. *Tetrahedron Lett.* 2003; **44**: 2077 – 2079.
16. Shen J, Shao J, Ou Zh, E W, Koszarna B, Gryko DT, Kadish KM. *Inorg. Chem.* 2006; **45**: 2251 – 2265.
17. Ou Zh, Shen J, Shao J, E W, Galenzowski M, Gryko DT, Kadish KM. *Inorg. Chem.* 2007; **46**: 2775 – 2786.
18. Shen J, Ou Zh, Shao J, Galenzowski M, Gryko DT, Kadish KM. *J. Porph. Phthal.* 2007; **11**: 269 – 276.
19. Ou Zh, Sun H, Zhu W, Da Z, Kadish KM. *J. Porph. Phthal.* 2008; **12**: 1 – 10.
20. Presselt M, Dehaen W, Maes W, Klamt A, Martinez T, Beenken WJD, Kruk M. *Phys. Chem. Chem. Phys*. 2015; **17**: 14096 – 14106.
21. Röder B, Büchner M, Rückman I, Senge MO. *Photochem. Photobiol. Sci*. 2010; **9**: 1152 – 1158.
22. Senge MO, MacGovan SA, O'Brien J. *Chem. Commun.* 2015; **51**: 17031 – 17063.
23. Capar J, Conradie J, Beavers CM, Ghosh A. *J. Phys. Chem. A*. 2015; **119**: 3452 – 3457.
24. Klenitsky DV, Kruk MM, Maes W. *Trudy BGTU* [Proceedings of Belarusian State Technological University (BSTU)] *Ser. 2, Chem. Engin., Biotechn., Geoecol., no. 1*. 2017; 23-28 (in Russian).
25. Kruk MM, Klenitsky DV, Maes W. *Trudy BGTU* [Proceedings of Belarusian State Technological University (BSTU)] *Ser. 3, Phys. Math. and Comp. Sci., no.1*. 2018; 36–42 (in Russian).
26. Broadhurst MJ, Grigg R, Shelton G, Johnson AW. *J. Chem. Soc. Perkin 1* 1972; 143 – 151.
27. Grigg R, Hamilton RJ, Jozefowicz ML, Rochester CH, Terrrel RJ, Wockwar H. *J. Chem. Soc. Perkin Trans. 2* 1973; 407 – 413.
28. Maes W, Ngo TH, Vanderhaeghen J, Dehaen W. *Org. Lett.* 2007; **9**: 3165 – 3168.
29. Ngo TH, Puntoriero F, Nastasi F, Robeyns K, Van Meervelt L, Campagna S, Dehaen W, Maes W. *Chem. Eur. J.* 2010; **16**: 5691 – 5705.
30. Maes W, Ngo TH, Rong G, Starukhin AS, Kruk MM, Dehaen W. *Eur. J. Org. Chem.* 2010; 2576 – 2586.
31. Gordon AJ, Ford RA. *The Chemist's Companion. A Handbook of Practical Data, Techniques and References*. Wiley-VCH: New York, 1972; 231 – 235.
32. Beenken W, Presselt M, Ngo TH, Dehaen W, Maes W, Kruk M. *J. Phys. Chem. A*. 2014; **118**: 862 – 871.
33. Klenitsky DV, Kruk MM. *Trudy BGTU* [Proceedings of Belarusian State Technological University (BSTU)] *no. 4: Chem., Technol. Org. Subst. and Biotechnol*. 2015; **177**: 20 – 23 (transl. into English).
34. Laikov DN. *Chem. Phys. Lett.* 1997; **281**: 151 – 156.
35. Laikov DN, Ustynyuk YuA. *Russian Chem. Bull*. 2005; **54**: 820 – 826.
36. Starukhin AS, Kruk MM, Gladkova OL, Maes W. *Macroheterocycles* 2011; **4**: 85 – 88.
37. Kruk MM, Ngo TH, Verstappen P, Starukhin AS, Hofkens J, Dehaen W, Maes W. *J. Phys. Chem. A*. 2012; **116**: 10695 – 10703.
38. Ajeeb YH, Karlovich TB, Gadkov LL, Maes W, Kruk MM. *J. Appl. Spectr*. 2019; **86**: 389 – 395.

39. Kielmann M, Senge MO. *Angew. Chem. Int. Ed*. 2019; **58:** 418 – 441.
40. Roucan M., Kielmann M, Connon SJ, Bernhard SSR, Senge MO. *Chem. Commun.* 2018; **54**: 26 – 29.
41. Knuykshto VN, Ngo TH, Dehaen W, Maes W, Kruk MM. *RSC Adv.* 2016; **6**: 43911 – 43915.
42. Kruk MM, Klenitsky DV, Gladkov LL, Maes W. *Trudy BGTU* [Proceedings of Belarusian State Technological University (BSTU)] *Ser. 3, Phys. Math. and Comp. Sci., no.1*. 2019; 6 – 13 (in Russian).

Table 1. Calculated pyrrole tilting angles φ and Δ23 values for the free base H_3AB_2 and unsubstituted corrole in the ground singlet S_0 and lowest triplet T_1 states.

Parameter	Compound							
	H_3AB_2 corrole				Unsubstituted corrole			
	T1 tautomer		T2 tautomer		T1 tautomer		T2 tautomer	
	S_0	T_1	S_0	T_1	S_0	T_1	S_0	T_1
φ_A, °	19.0	21.9	19.3	24.1	16.3	20.2	17.4	21.6
φ_B, °	11.4	25.0	7.3	14.7	7.5	14.1	3.7	9.3
φ_C, °	5.6	11.4	3.9	4.0	3.8	4.0	2.1	1.6
φ_D, °	6.7	4.5	5.4	1.8	5.9	1.9	3.3	3.4
Δ23, Å	0.200	0.330	0.198	0.246	0.163	0.209	0.152	0.204

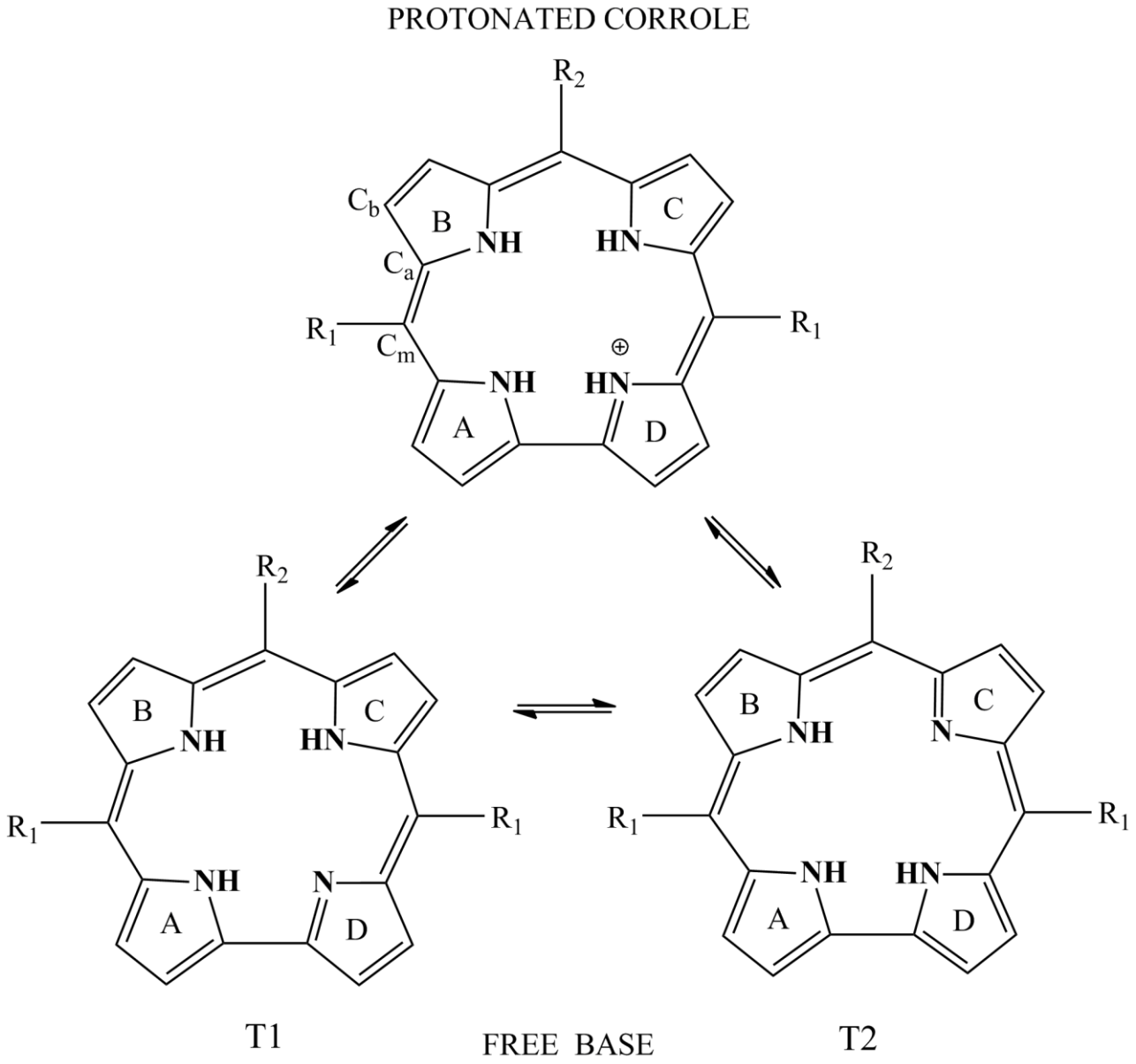

Fig. 1. Acid-base equlibria in free base corroles. R_1 = mesityl and R_2 = 4,6-dichloropyrimidinyl relate to the substituents of the corrole molecule studied in this paper. Capital letters from A ot D denote the pyrrole rings as they are referred to in the text.

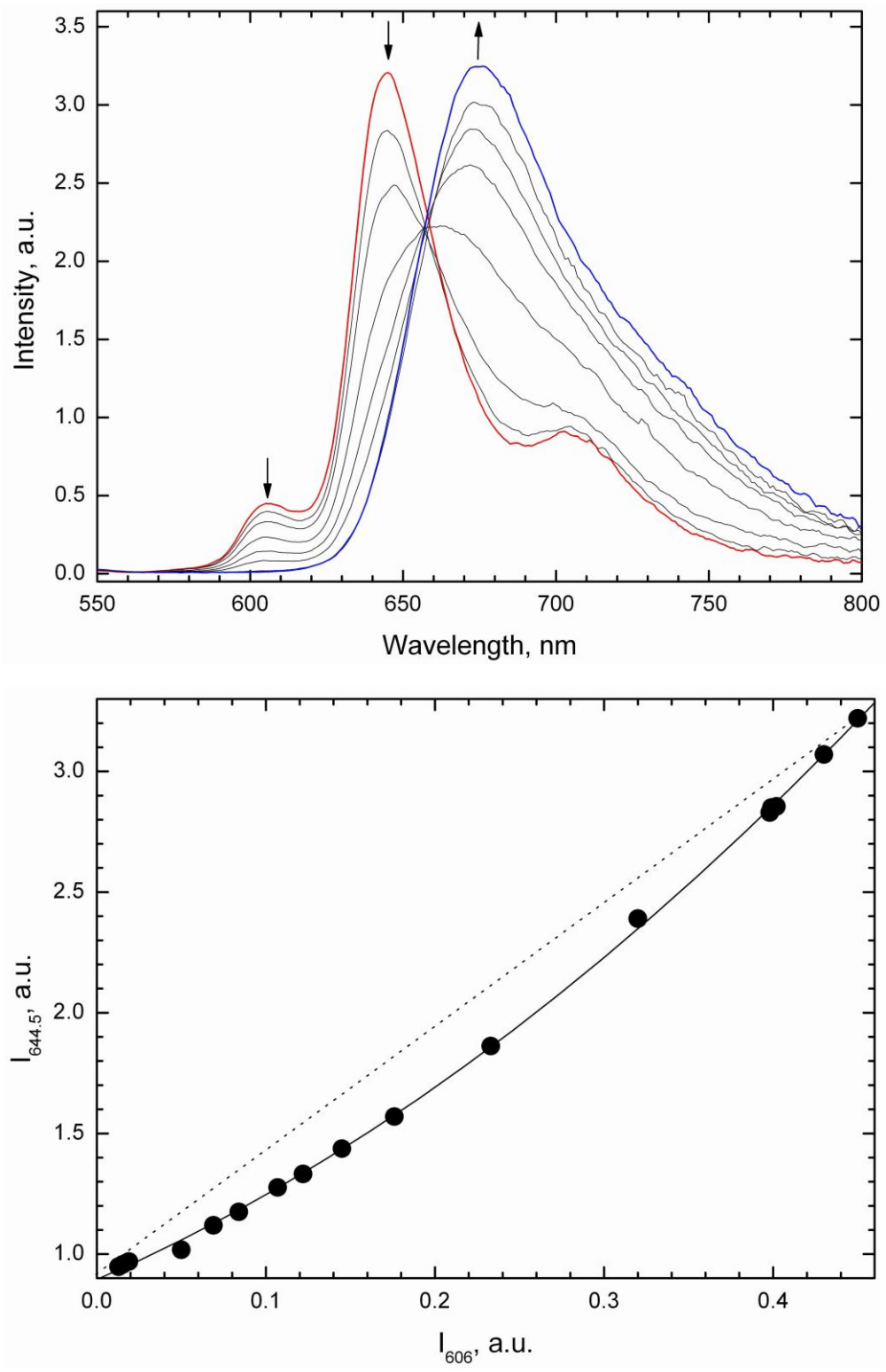

Fig. 2. (top) Fluorescence spectra of the H_3AB_2 *meso*-pyrimidinylcorrole measured over the course of the titration with H_2SO_4 in ethanol (λ_{exc} = 465 nm). Arrows indicate the direction of intensity changes during the titration. (bottom) Intensity vs. intensity plot demonstrating the changes in the proportion between the excited singlet S_1 state concentrations of the two NH tautomers over the course of the titration. The dotted straight line indicates the hypothetic proportion when the two corrole NH tautomers are protonated at the same rate. See text for details.

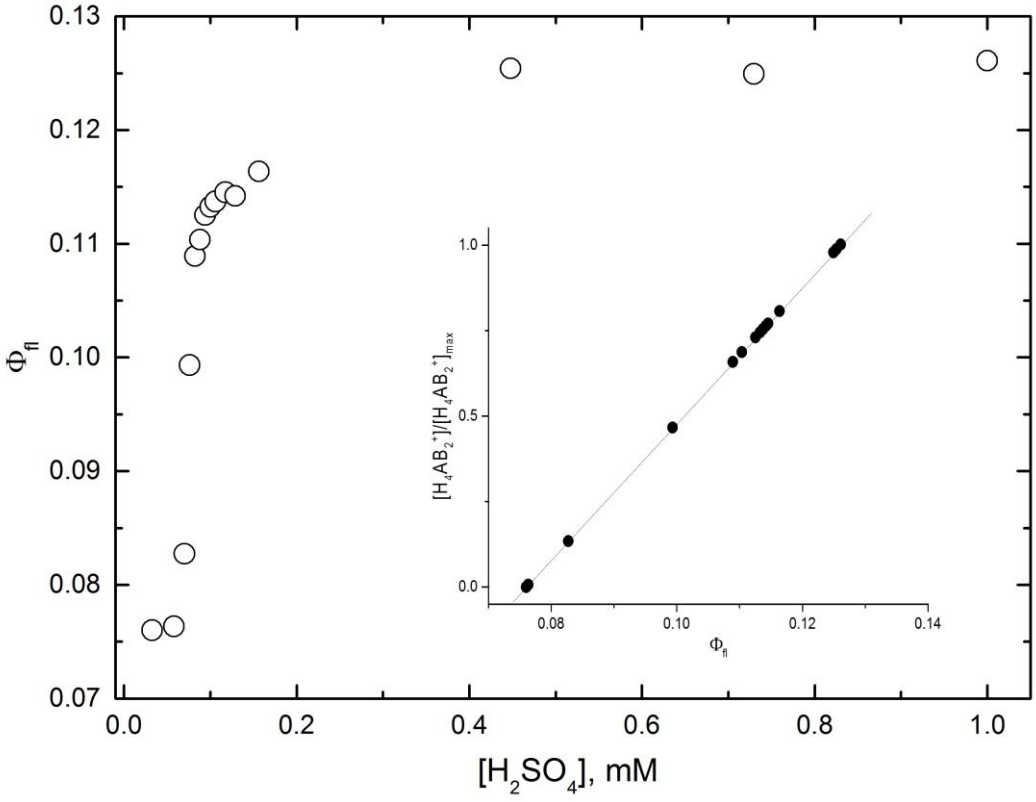

Fig. 3. Dependence of the fluorescence quantum yield Φ_{fl}, measured over the course of the titration of H_3AB_2 *meso*-pyrimidinylcorrole, on the acid concentration in solution. The inset shows the calculated relationship between the fluorescence quantum yield and the relative amount of protonated $H_4AB_2^+$ corrole during the titration.

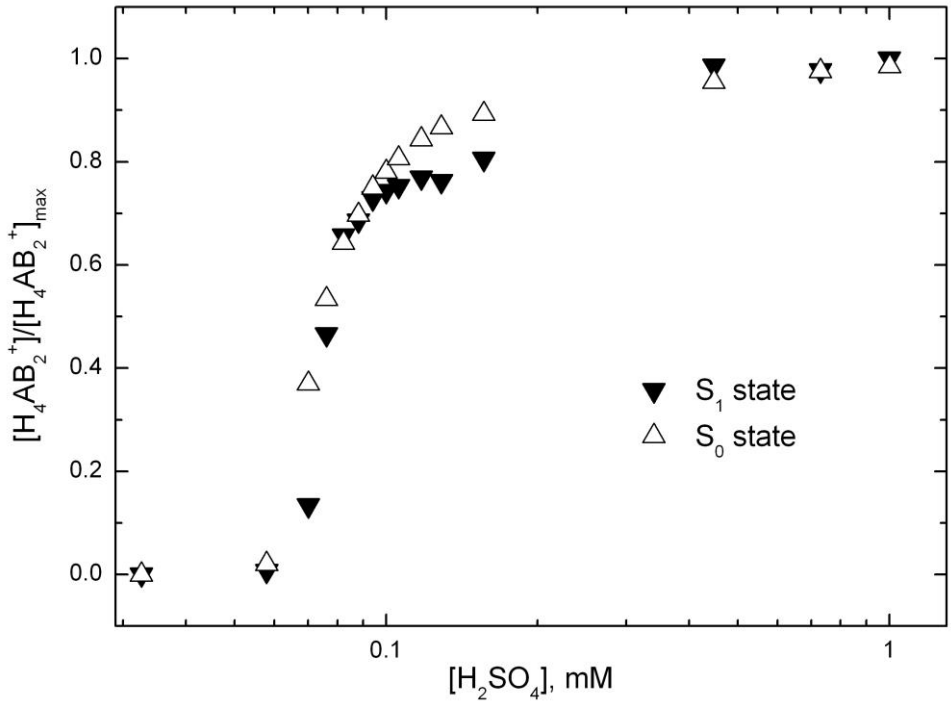

Fig. 4. Relative amount of protonated $H_4AB_2^+$ corrole in the ground singlet S_0 (△) and lowest excited S_1 (▼) states as a function of acid concentration in solution.

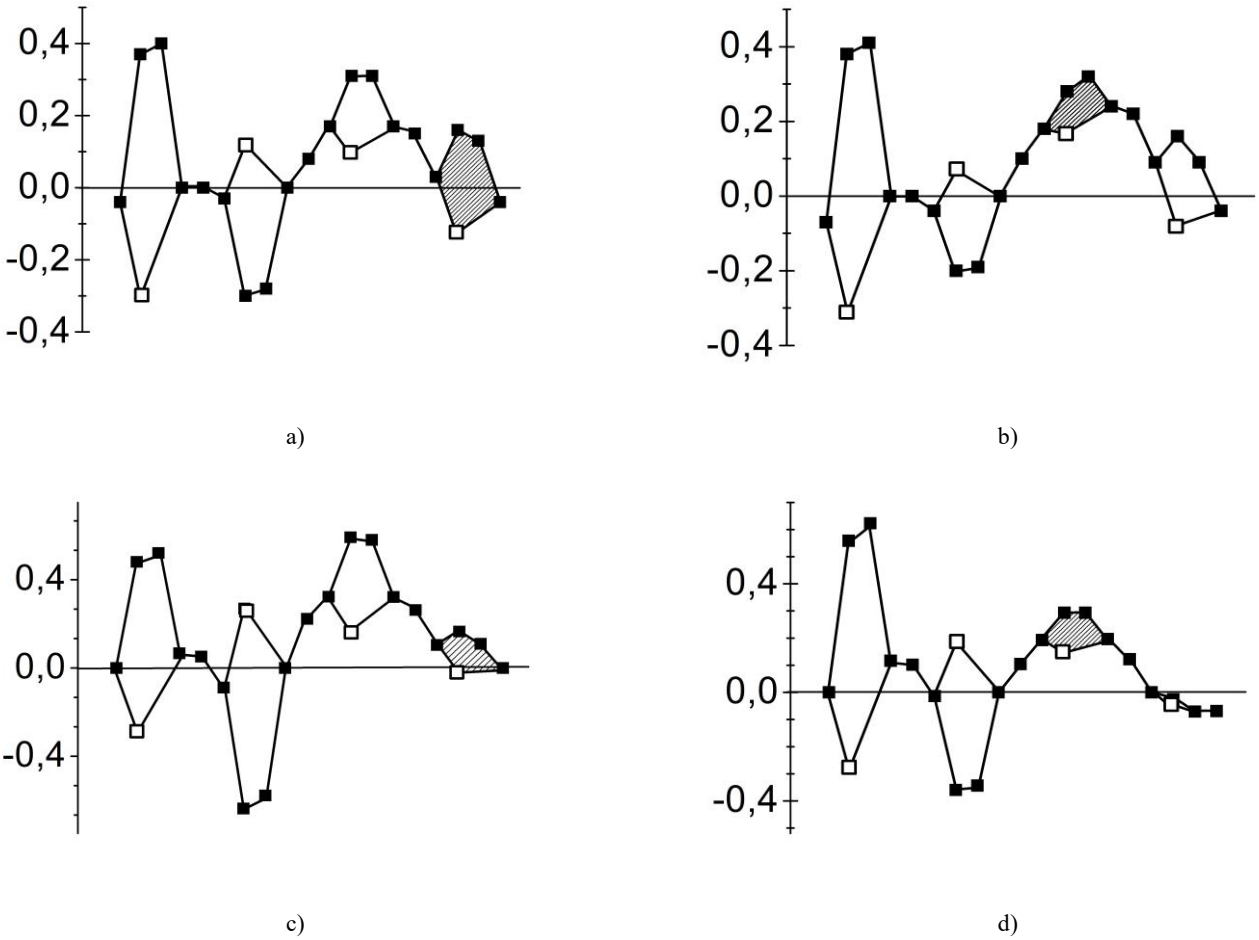

Fig. 5. Diagram of atom deviations from the macrocycle mean plane for 10-(4,6-dichloropyrimidinyl)-5,15-dimesitylcorrole (in Å): a,b) T1 and T2 tautomers in the ground singlet S_0 state; c,d) T1 and T2 tautomers in the lowest excited triplet T_1 state. Pyrrole rings A, B, C and D are counted from left to right and the pyrrole rings to be protonated are shaded.

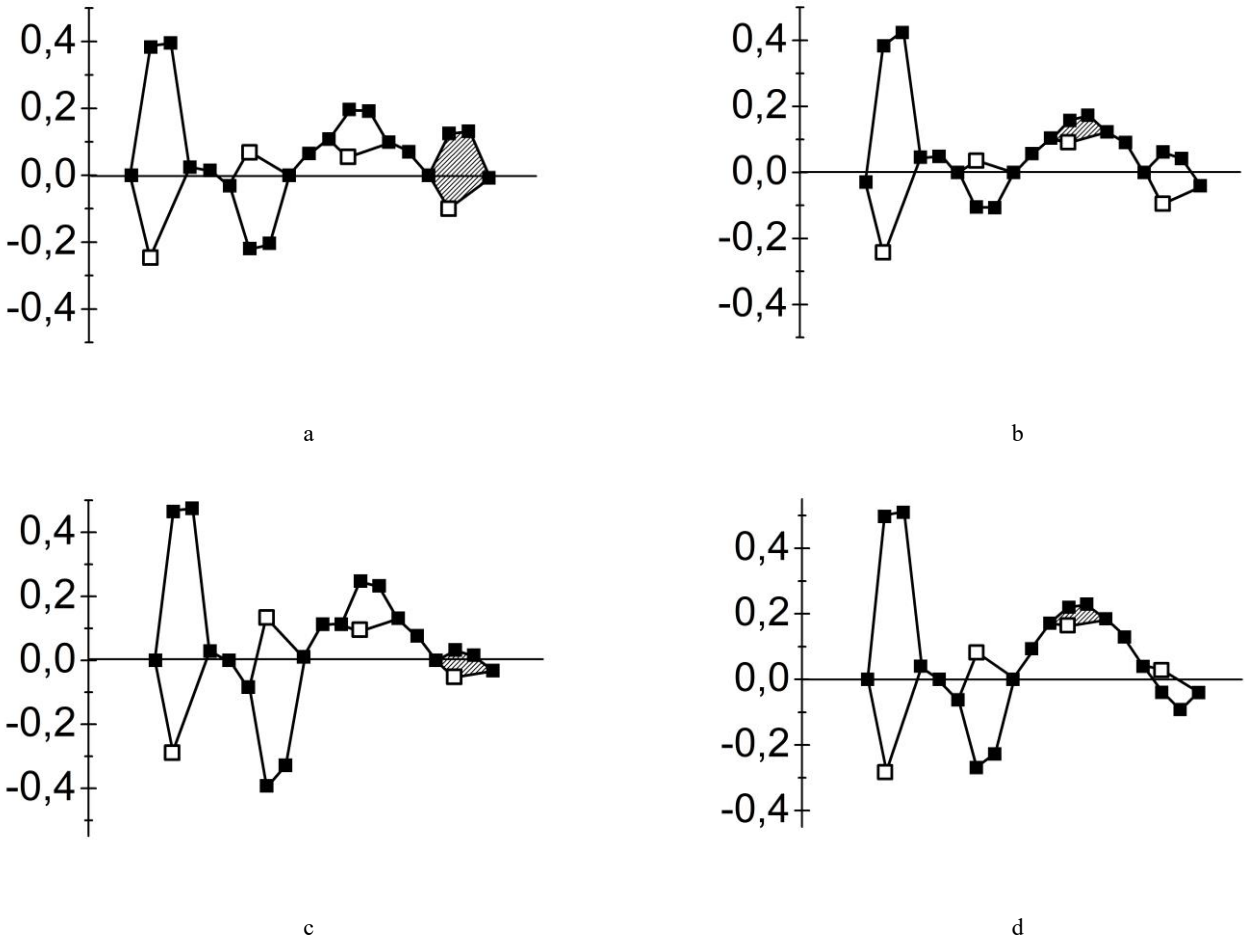

Fig. 6. Diagram of atom deviations from the macrocycle mean plane for the unsubstituted free base corrole (in Å): a,b) T1 and T2 tautomers in the ground singlet S_0 state; c,d) T1 and T2 tautomers in the lowest excited triplet T_1 state. Pyrrole rings A, B, C and D are counted from left to right and the pyrrole rings to be protonated are shaded.